2013 IEEE/RSJ International Conference on
Intelligent Robots and Systems (IROS)
November 3-7, 2013. Tokyo, Japan

Development of Crane Tele-operation System using Laser Pointer Interface

Masaki Negishi[1], Hisasi Osumi[2], Keiichirou Saito[1], Hikaru Masuda[1], Yusuke Tamura[2]

Abstract—**A teleoperation system for a crane is developed. The crane uses a small actuator and large actuator in each direction (x and y). The large actuator is controlled by input signals from a laser pointer interface, and the small actuator is used as a regulator and is feedback-controlled by a wire angle sensor. To avoid overshoots in the suspended object at the target point and to eliminate the effect of the trembling of the irradiated light by the laser pointer, the velocity commands sent to the large actuator are designed by accumulating cubic functions, each of which is based on the displacement of the irradiated light in a sampling period. The effectiveness of the developed control system and its control algorithm were verified through experimental results.**

I. Introduction

Wire suspension systems, including overhead cranes, are frequently used in factories because a crane can transport suspended objects in a three-dimensional space. However, because of the characteristics of cranes, pendulum vibration occurs during the transportation of suspended objects. This pendulum vibration must be controlled because it can lead to load collapse. Moreover, the method used to stop objects with residual vibration not only degrades the work efficiency but can also cause accidents, including load shifting. Therefore, operators must have advanced operation skills.

One of the solutions to this problem is to automate the vibration control and transportation by cranes. However, the existing studies have only treated two issues: the trajectory generation and suppression of pendulum vibration using feedback control or feedforward control [1][2]. To control pendulum vibration, a transportation method that considers jerk has been proposed. Yet, this method does not take the hoisting wire into account. Moreover, these studies [3][4][9] did not consider three-dimensional transportation. On the other hand, the studies on teleoperation systems have mainly proposed operation interfaces. Therefore, no method has previously been proposed to control the pendulum vibration that results from disturbance and overshooting at the target point. To improve the readiness and positioning precision, the authors developed a two-stage servo system. This system consists of a small actuator and large actuator for each direction (x and y). The large actuator is controlled by operator commands, and the small actuator is controlled by feedback signals obtained by wire angle sensors. Moreover, we invented an operation interface and developed a system that facilitates control of pendulum vibration caused by disturbance and overshoots at the target point.

In this paper, we proposed an operational system that uses a laser pointer. The operator can give an instruction directly to the crane in the system. Furthermore, its effectiveness was verified through an experiment. We expect that this system could be used, not only for large cranes in factories, but also for a lift traveling along the ceiling of a care facility.

First, an overview of the developed crane teleoperation system is provided in section II. Then, a control algorithm for the macro-micro servo system is described in section III. In section IV, the operation interface that we developed is presented. Section V discusses how the effectiveness of the proposed system was verified through an experiment.

II. Overview of Teleoperation System

The structure of the developed crane and the system configuration are shown in Fig. 1 and Fig. 2, respectively. The crane moves freely in a two-dimensional plane (x and y). The crane comprises a two-stage servo system. There is a large actuator and a small actuator for each axis. The system is introduced in series using a movable table with a ball screw. The large actuator is used to transport suspended objects, and the small actuator controls the pendulum vibration. Therefore, this crane can respond to high-frequency disturbance. In addition, the small actuator has a wire winding mechanism. This mechanism is used for obstacle avoidance. DC servomotors are used in these five actuators and control the speed. Each motor includes an encoder that detects the position of the crane and the height of the suspended object with high accuracy. In addition, a camera is attached to the crane. Therefore, we can obtain images around the suspended object from directly above. The teleoperation of the crane is accomplished by clicking on points in an image, as shown in a previous research [8]. In this study, the operator irradiates a goal point with a laser, and the amount of laser light is measured by the camera to generate a control input.

III. Control Laws of Two-Stage Servo System

A. *Control model of crane*

The x- and y-axes are orthogonal to each other, and we assume that the swinging motion of the suspended mass is small enough to neglect the coupling effect in the x- and y-directions. Therefore, the large actuator and small actuator can be modeled independently in the two-dimensional plane.

[1]K. Saito, M. Negishi, and H. Masuda are with the Course of Precision Engineering, Graduate School of Science and Engineering, Chuo University, 1-13-27 Kasuga, Bunkyo, Tokyo 112-8551, Japan

[2]H. Osumi and Y. Tamura are with the Department of Precision Mechanics, Faculty of Science an Engineering Chuo University, 1-13-27 Kasuga, Bunkyo, Tokyo 112-8551, Japan

A simple model in the x-z plane is shown in Fig. 3. The equations of motion for the small actuator, large actuator, and suspended object are expressed in equations (1), (2), and (3), respectively.

$$F_f = (M_f + m)(x_c + \ddot{x}_f) + \{(2l\ddot{\varphi}_x + l\ddot{\varphi}_x)\cos\varphi_x + (\ddot{l} - l\ddot{\varphi}_x^2)\sin\varphi_x\} \quad (1)$$

$$F_c = M_c\ddot{x}_c + F_f \quad (2)$$

$$ml^2\ddot{\varphi}_x = -2ml\dot{l}\dot{\varphi}_x - ml(\ddot{x}_c + \ddot{x}_f\cos\varphi_x) - mgl\sin\varphi_x \quad (3)$$

The parameters of these equations are shown in Fig. 3. M_c is the mass of the moving part of the large actuator, M_f is the mass of the small actuator, and g is the gravitational acceleration. The control input is the force generated by the large actuator and small actuator. Setting the z-axis as the vertical direction, the suspended object has translational and rotational movement on the x- and y-axes. F_c and F_f are the forces generated by the large and small actuators, respectively. Equation (4) is the linear approximation result of equations (1), (2), and (3).

$$F_e = -\frac{g\varphi_x}{\ddot{x}_e} \quad (4)$$

Equation (4) shows that F_e , the force applied to the suspended object is proportional to the deflection angle. Because we cannot apply any force directly to the suspended object, we apply a pseudo-force to it by determining the deflection angle of the wire corresponding to the target input.

B. *Desired trajectory of suspended object*

From equations (3) and (4), the relationship between the position of the carrier and the moving table is shown in equation (5).

$$x_g = x_e + \frac{l}{g}\ddot{x}_e \quad (5)$$

Therefore, the velocity function of the crane must be physically continuous. In other words, a jerk in the position of the suspended object needs to be described as a continuous function. Thus, the target velocity is divided into three sections: an acceleration section, deceleration section, and constant velocity section. The acceleration section consists of two quadratic functions. These two quadratic functions generate a velocity trajectory that satisfies equation (5). As shown in Fig. 5, to simplify the formula of crane trajectory, motion commands for suspended object during acceleration and deceleration start from $-T_{acc}$. If the goal position given by the operator is changed during a displacement, the trajectory between the previous target point and the new one is calculated in the same manner, and the suspended object is transported toward the new target position via the previous target position. The duration of the acceleration and deceleration sections is $2T_{acc}$, where T_{acc} is set to 1 s. T_c is the duration of the constant velocity section. V_o is the constant velocity. The velocity is calculated using the distance from the initial point to the end point and the maximum velocity of the crane. In addition, α is the value of the jerk and is determined by T_{acc} and the initial and end velocities, as shown in equation (6).

$$\alpha = \frac{4V_0}{T_{acc}^3} \quad (6)$$

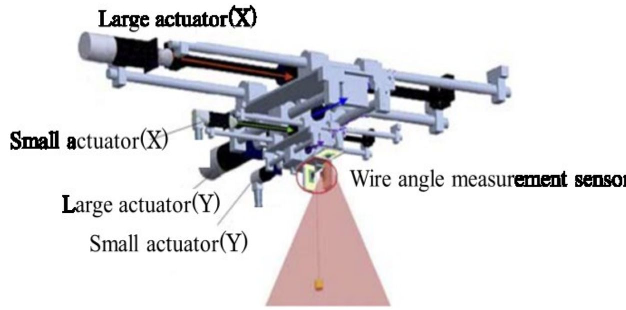

Fig. 1 Structure of developed crane

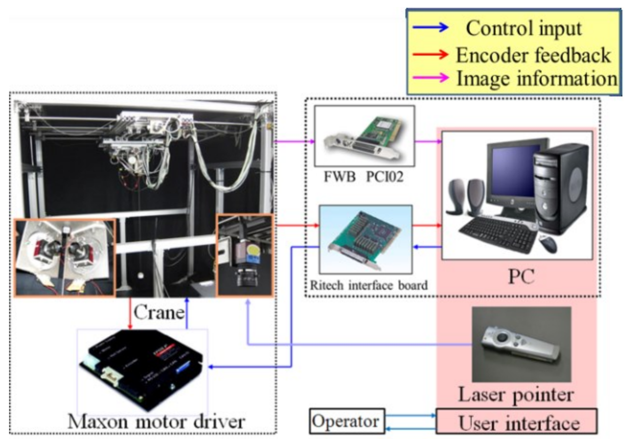

Fig. 2 Configuration of crane control system

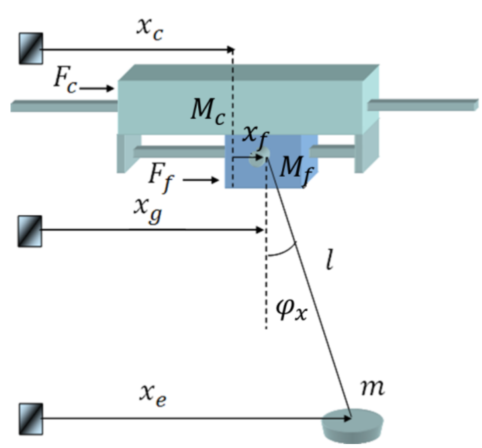

Fig. 3 Simplified dynamic model of crane system

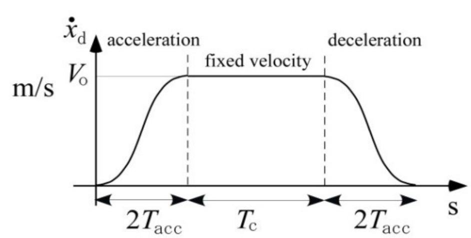

Fig. 4 Desired velocity of suspended object

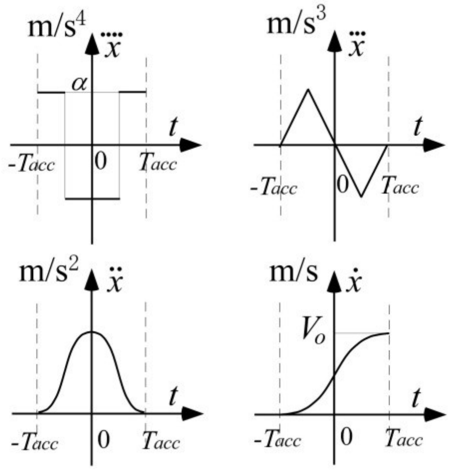

Fig.5 Motion commands for suspended object during acceleration and deceleration

C. *Control law for small actuator and large actuator*

The small actuators control the pendulum vibration caused by disturbances. The large actuators transport the suspended object. Therefore, the range of movement of each small actuator is narrow. Moreover, it is desirable to stay as close to the origin as possible. On the other hand, the large actuators must follow a given trajectory, as shown in equation (5), without delay or deviation. Each desired trajectory is determined by equations (7) and (8), where subscript d indicates the desired value.

$$x_{fd} = 0 \tag{7}$$

$$x_{cd} = x_{gd} \tag{8}$$

Regulators are used for the small actuators to achieve equations (7) and (8). Because the deflection angle is needed to control the suspended object, based on equation (3), we adopt a regulator whose equilibrium point shifts with the drive of the large actuator. The target deflection angle obtained from equation (3) is shown in equation (9). The state equation of the system is shown in equation (10). If the wire length is changed by hoisting, the pendulum period is changed. Therefore, equation (10) considers the velocity component of the wire length to cope with a change in the wire length.

$$\varphi_{cd} = -\frac{\ddot{x}_{ed}}{g} \tag{9}$$

$$\begin{bmatrix} \dot{x}_f \\ \ddot{x}_f \\ \dot{\varphi}_x - \dot{\varphi}_{xd} \\ \ddot{\varphi}_x - \ddot{\varphi}_{xd} \end{bmatrix} = \begin{bmatrix} 0 & 1 & 0 & 0 \\ 0 & 0 & 0 & 0 \\ 0 & 0 & 0 & 1 \\ 0 & 0 & -g/l & -2\,\dot{l}/l \end{bmatrix} \begin{bmatrix} x_f \\ \dot{x}_f \\ \varphi_x - \varphi_{xd} \\ \dot{\varphi}_x - \dot{\varphi}_{xd} \end{bmatrix} + \begin{bmatrix} 0 \\ 1 \\ 0 \\ -1/l \end{bmatrix} u_a \tag{10}$$

u_a is the state feedback, which shifts its equilibrium point, as shown in equation (11).

$$u_a = f\begin{bmatrix} x_f & x_f^2 & \varphi - \varphi_d & \dot{\varphi} - \dot{\varphi}_d \end{bmatrix}^T \tag{11}$$

This feedback gain, f, can be designed using the pole placement method. The system sets the pole at $-2.57 \pm 1.86\,j, -1.01 \pm 2.96\,j$, and the feedback gain is calculated and controlled momentarily according to the wire length. Therefore, if the wire length changes, the swing of the suspended object converges at the same pole. The large actuator is controlled by the velocity control system. The acceleration is freely controlled by changing the target velocity. Accordingly, an acceleration input given to the moving table can be described as equation (12).

$$\ddot{x}_c = u \tag{12}$$

Here, the acceleration input is shown in equation (13).

$$u = \ddot{x}_{cd} + K_v(\dot{x}_{cd} - \dot{x}_c) + K_l(x_{cd} - x_c) \tag{13}$$

where K_v and K_l are proportional gains. Equation (14) is the state equation derived from equations (12) and (13), if the error of the target input and output is $e = (x_{cd} - x_c)$,

$$\begin{bmatrix} \dot{e} \\ \ddot{e} \end{bmatrix} = \begin{bmatrix} 0 & 1 \\ -K_l & -K_v \end{bmatrix} \begin{bmatrix} e \\ \dot{e} \end{bmatrix} \tag{14}$$

If we properly select the proportional gain, the system can converge arbitrarily. When the wire length changes, the reaction force affects the actuator. However, if the speed control of the motors is designed appropriately, the developed control system can be used directly. This is why a change in the reaction force is caused by a change in the wire length. Even if the power is temporarily degraded, it immediately follows the target trajectory.

IV. Development of Operation Interface

A. Overview of target position input by laser pointer

Figure 6 shows how to operate the developed crane system. An operator who is close to the suspended object uses a laser pointer to target the location where he wants to transport the object. Potential target locations are specific points or objects on the floor. The irradiated point is detected by the camera that is attached to the top of the crane and pointed in a downward direction. Feedback control is conducted as the crane follows the irradiation point. At that time, the crane not only follows the last irradiation point, but also transports the object along the trajectory of the laser light as far as possible. Furthermore, when the laser light passes a high obstacle, the system can measure the height of the obstacle using motion stereo. Therefore, the wire is automatically hoisted to a height that allows the suspended object to avoid the obstacle. Then, the stop position of the laser light or the position where the laser light finally disappears is determined to be the final target stop position.

B. Generation of target trajectory of suspended object

There are two problems in realizing the above system, in which a laser pointer is used as an input device. The first is how to generate a target trajectory without overshoot, and the other is how to avoid instability in the irradiation point from hand movement. The following method is adopted as a countermeasure to these problems.

First, the irradiation position of a laser pointer and the target point of the suspended object are measured at each sampling time ΔT, as shown in Fig. 7(a). In this system, the sampling time is 30 ms. P_{i+1} denotes a measure point at the (i+1)-th control sampling point, and each increment in the x- and y-directions for the i-th sampling is Δx_i and Δy_i, respectively. Based on the calculated travel distance, the target velocity trajectory is generated, as shown in Fig. 4. However, the displacement in ΔT is small enough to ignore the constant velocity section shown in Fig. 4. The target velocity trajectory in the x-direction is shown in Fig. 7(b). The target velocity trajectory in the y-direction is the same as that in the x-direction. The travel time, $4T_{acc}$, is the sum of the acceleration and deceleration times. The velocities for the displacements in the x- and y-directions are V_{ox} and V_{oy}, respectively, as shown in equations (15) and (16).

$$V_{ox} = \Delta x_i / 2T_{acc} \tag{15}$$

$$V_{oy} = \Delta y_i / 2T_{acc} \tag{16}$$

The velocity command is modified by superposing equations (15) and (16) on the current velocity command of the crane. As shown in Fig. 7(c), the superposed velocity trajectory ends at ΔT after the previous target arrival time. Therefore, the crane follows the target point while passing near the final target. In addition, in a case where the irradiation point of the laser light sways because of hand movement, the effect becomes negligibly small because the plus and minus effect is offset when the control order is summed up. The velocity of the crane helps achieve the superposition value shown in Fig. 7(c), which can exceed its maximum limitation. In this case, the system seeks the maximum value of the velocity by repeatedly displacing the final target arrival time backward by ΔT, and the superposition is performed only when the velocity is slower than the maximum velocity of the crane. This situation occurs when the velocity of the laser pointer is higher than that of the crane. Thus, a method that makes the travel time of the crane longer than that of the laser pointer is reasonable. Moreover, if an operator uses a laser pointer around a crane that remains stationary, the velocity waveform of the crane is shown in Fig. 7(d). In this case, the trajectory of the velocity, as shown in Fig. 7(b), is continuously generated for each sampling time. This velocity trajectory is shown in Fig. 7(b). Moreover, in this case, when the maximum target velocity exceeds the maximum velocity of the crane, the same control algorithm as shown in Fig. 7(c) can be applied.

V. Experiment

A. Parameters

The parameters of the developed system are listed in Table 1. There is a gap between the sampling time of the control system and that of the camera. Until a new image is obtained, the system calculates using the previous image.

B. Experimental procedure

The proposed control law was applied to the developed system, and we conducted an experiment to transport a suspended object using the system. The experiment was roughly divided into the following three phases.

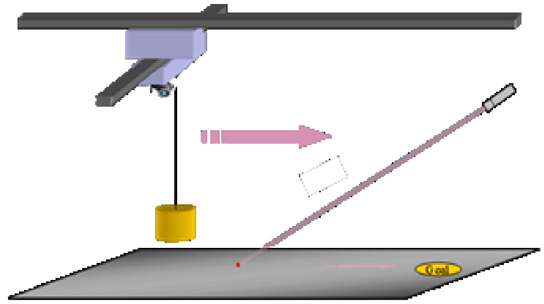

Fig. 6 Method for indicating target location using laser pointer

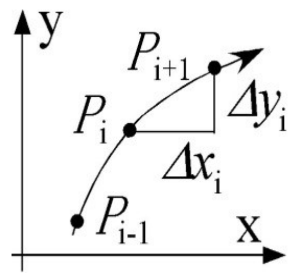

(a) Sampling point

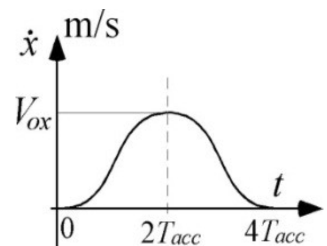

(b) Generated trajectory

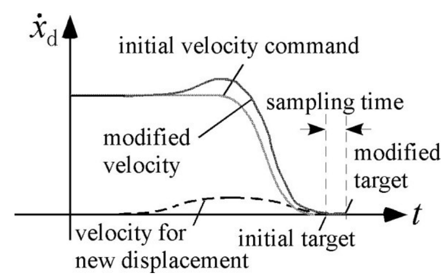

(c) Modified command by latest sampling

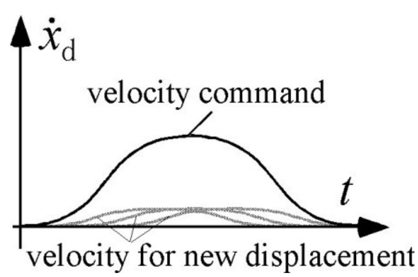

(d) Velocity command consisting of each sampling

Fig. 7 Crane motion command based on target position

1) Verification of the effect of the pole placement method

The crane transported suspended objects in the x-axis direction using wire hoisting. At that time, the vibration suppression performance of the proposed control law was compared with that of the case in which the feedback gain was fixed. The initial length of the wire was 1.37 [m], and the initial height of the suspended object from the ground was 0.3 [m].

2) Verification of the effectiveness of the laser pointer system

An operator drew a circular trajectory, as shown in Fig. 8, and the crane followed this trajectory. It took us 13.9 [s] to transport it around the circular trajectory. At this time, the velocity of the crane corresponded to Fig. 7(d).

3) Verification of the ability to follow a three-dimensional target trajectory

As shown in Fig. 9, an obstacle was placed along the travel direction. The start and goal points were connected by a straight line using a laser pointer, and laser light was irradiated over the obstacle. Here, the winding operation was conducted using the experimenter's button operations. The height of the obstacle was 0.5 [m], and the transportation distance was 0.94 [m].

C Experimental results

1) The variation in the wire length is shown in Fig. 10, and the variation in the feedback gain using the pole placement method is shown in Fig. 11. The deflection angle of the wire is shown in Fig. 12. As shown in Fig. 12, the pendulum vibration was controlled after hoisting the wire. Therefore, we confirmed that the system could adapt to changes in the pendulum vibration cycle.

2) The transportation location is shown in Fig. 9. The transportation results for each axial direction component are shown in Fig. 10. As shown in Fig. 9, the target trajectory was generated smoothly. Therefore, the hand movement of the laser pointer had little effect on the target trajectory generation, and we confirmed that a suspended object could follow the target trajectory. As shown in Fig. 10, the suspended object followed the target trajectory with no time lag in either axial direction. We also confirmed that the suspended object could stop at the target position with no overshoot or steady-state error.

3) A trajectory where the suspended object had to avoid an obstacle is shown in Fig. 11. The altitudinal resolution depended on the wire length and the velocity of the crane. In this system, the altitudinal resolution was about 10 [mm]. As shown in Fig. 11, the suspended object could avoid the obstacle by hoisting the wire. Even if the height of the irradiation point changed erratically, the target trajectory was measured correctly. At that time, we confirmed that the suspended object did not experience pendulum vibration. In addition, the suspended object followed close to the critical point.

Table 1 Parameters of crane system

	Large actuator		Small actuator	
	X	Y	x	y
Working distance [mm]	1200	900	200	200
Positioning resolution [μm]	12.5	8.0	1.5	1.5
Maximum velocity [m/s]	1.66	1.03	0.38	0.38
Angle resolution : 0.002 [rad]	Wire length : 0.26~1.62 [m]			
Pos. res. of mass : 2.0 [mm]	Suspended mass : 1.0 [kg]			
System sampling time : 30 [ms]	Camera sampling time : 50 [ms]			
T: 1.0 [s]	V_{max}: 0.3 [m/s]			
Poles of regulator	$-2.57\pm1.86i$, $-1.01\pm2.96i$			

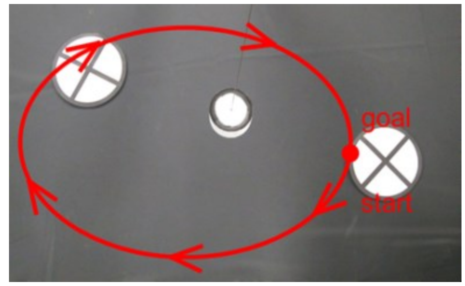

Fig. 8 Overview of transportation area

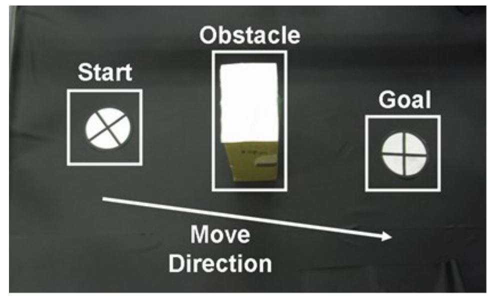

Fig. 9 Overview of transportation area containing obstacle

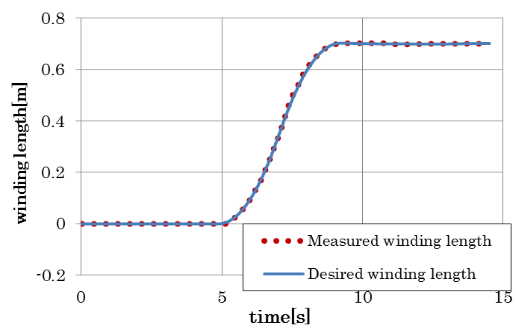

Fig.10 Variation of wire length

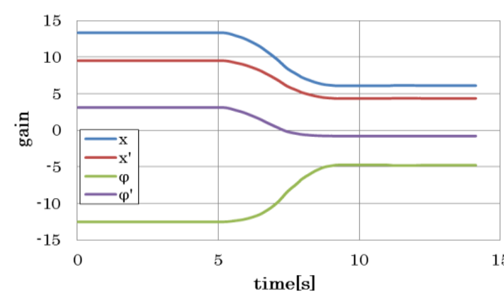

Fig. 11 Feedback gain

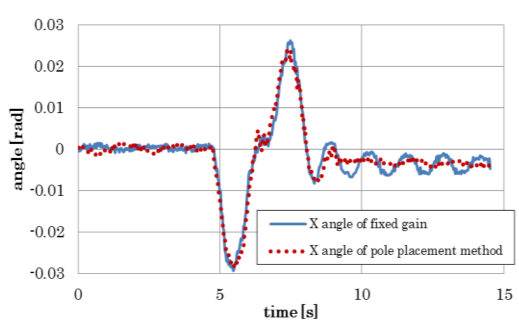

Fig. 12 Measured wire angle with hoisting

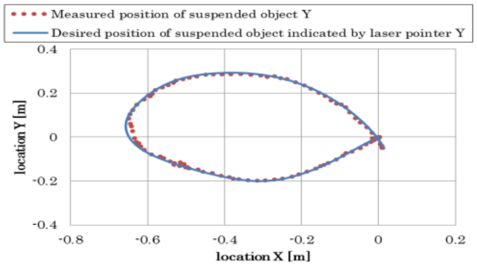

Fig. 13 Locus of suspended object when using laser pointer

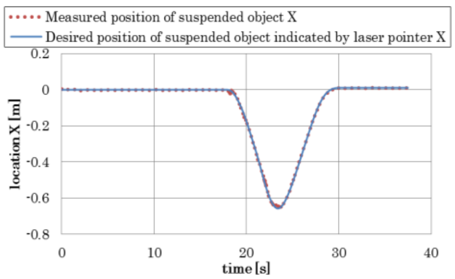

x-direction

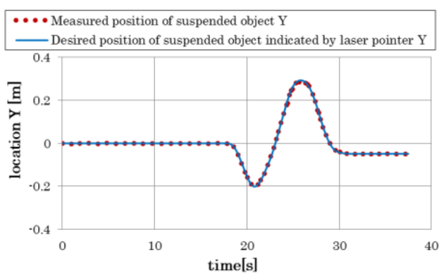

y-direction

Fig. 14 Observed position of suspended object when using laser pointer

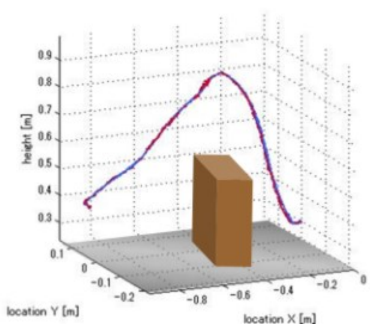

Fig. 15 Locus of suspended object during transportation

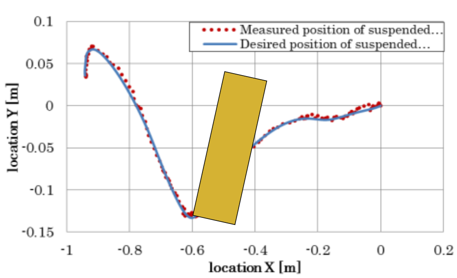

Fig. 16 Measured position of suspended object during transportation

VI. Conclusion

In this study, we considered the winding operation for a suspended object and proposed a vibration control method using the pole placement method. Moreover, we developed an operation that uses a laser pointer. The developed control system and operation interface were applied to an experimental system. To confirm the effectiveness of the proposed methods, we conducted a transportation experiment. The results of this experiment demonstrated that the developed laser pointer interface systems were effective for transportation in an area with obstacles. We also demonstrated that an operator could intuitively control and transport an object to a target point with high accuracy. In future work, winding automation will be conducted. The effect of illumination change at the scene and the shape of the suspended object will also be considered.

References

[1] H. Aschemann, O. Sawodny, S. Lahres, E.P. Hofer, "Disturbance Estimation and Compensation for Trajectory Control of an Overhead Crane," *Proceedings of the American Control Conference*, pp.1027-1031, 2000.

[2] W. Sridokbuap, S. Nundarkwang, T. Benjanarasuth, J. Ngamwiwit, N. Komine, "I-PD and PD Controllers Designed by CRA for Overhead Crane System," *Proceedings of the International Conference on Control, Automation and Systems*, pp.326-330, 2007.

[3] N. Sun, Y. Fang, X. Zhang, Y. Yuan, "Phase Plane Analysis Based Motion Planning for Underactuated Overhead Cranes," *Proceedings of the 2011 IEEE international Conference on Robotics and Automation*, pp.3483-3488, 2011.

[4] N. Sun, Y. Fang, X. Zhang, Y. Yuan, "Transportation Task-Oriented Trajectory Planning for Underactuated Overhead Cranes using Geometric Analysis" *IET Control Theory and Applications*, Vol.6, No.10, pp.1410-1423, 2012.

[5] M. Yoneda, F. Arai, T. Fukuda, K. Miyata, T. Naito, "Operational Assistance System for Crane using Interactive Adaptation Interface-Design of 3D Virtual Crane Simulator for Operation Training," *Proceedings of the 6th IEEE International Workshop on Robot and Human Communication*, pp.224-229, 1997.

[6] K.C.C. Peng, W.E. Shighose, S. Gessesse, D. H. Frakes, "Crane Operation using Hand-Motion and Radio Frequency Identification Tags," *Proceedings of the IEEE International Conference on Control and Automation*, pp.1110-1115, 2009.

[7] H. Osumi, A. Miura, S. Eiraku, "Positioning of Wire Suspension System using CCD Cameras," *Proceedings of the 2005 IEEE/RSJ International Conference on Intelligent Robots and Systems*, pp.1665-1670, 2005.

[8] H. Osumi, M. Kubo, S. Yano, K. Saito, "Development of Tele-Operation System for a Crane without Overshoot in Positioning," *Proceedings of the 2010 IEEE/RSJ International Conference on Intelligent Robots and Systems*, pp.5799-5805, 2010.

[9] N. Sun, Y. Fang, Y. Zhang, Bojun Ma, A Novel Kinematic Coupling-Based Trajectory Planning Method for Overhead Crane, IEEE/ASME Transactions on Mechanics, vol. 17, no.1, pp. 166-173,Feb. 2012.